Earth, Planets and Space

FULL PAPER Open Access

Solar activity dependence for the relationship between nighttime medium-scale traveling ionospheric disturbance and sporadic E (*Es*) layer activities in summer during 1998–2019 over Japan

Veera Kumar Maheswaran[1], Yuichi Otsuka[2], James A. Baskaradas[1*], Venkata Ratnam Devanaboyina[3], Sriram Subramanian[1], Atsuki Shinbori[2], Takuya Sori[2], Michi Nishioka[4] and Septi Perwitasari[4]

Abstract

To investigate solar activity dependence of the coupling between medium-scale traveling ionosphere disturbance (MSTID) and sporadic E (*Es*) layer, we analyzed the total electron content (TEC) obtained from a Japanese global positioning system (GPS) receivers and ionosonde at Kokubunji (35.7° N, 139.5° E) in Japan during the summer period of May–August from 1998 to 2019. To obtain perturbation TEC caused by MSTIDs, the detrended TEC is calculated by subtracting 1-h moving averages from the measured TEC for each pair of GPS satellite and receiver. The detrended TEC data are mapped on to the geographical coordinates to make detrended 2-D maps with spatial resolution of 0.15°×0.15° in longitude and latitude. The MSTID activity is defined as a ratio of the standard deviation to the background TEC over Kokubunji in Japan. Day-to-day variations of the MSTID activity during summer nights was compared to *Es* layer parameters [critical frequency (f_oEs) and $\Delta f_{o-b} \equiv f_oEs - f_bE$, where f_bEs is blanketing frequency] derived from ionosonde station at Kokubunji. We have found that the correlation coefficient between the MSTID activity and $f_oEs(\Delta f_{o-b})$ between 1998 and 2019 is 0.5 3 (0.46) on average, suggesting that there is an electrodynamical coupling between the *Es* layer and F region could generate nighttime MSTIDs. We also have found that the correlation coefficient positively correlates with solar activity. This finding indicates that in the high solar activity conditions, when the growth rate of Perkins instability is relatively low, generation of the polarization electric fields in the *Es* layer could play a more important role to grow MSTIDs than in the low solar activity conditions.

Keywords TEC, MSTID, Sporadic E layer, Electrodynamical coupling, Solar activity

*Correspondence:
James A. Baskaradas
jamesbaskaradas@ece.sastra.edu
Full list of author information is available at the end of the article

Graphical Abstract

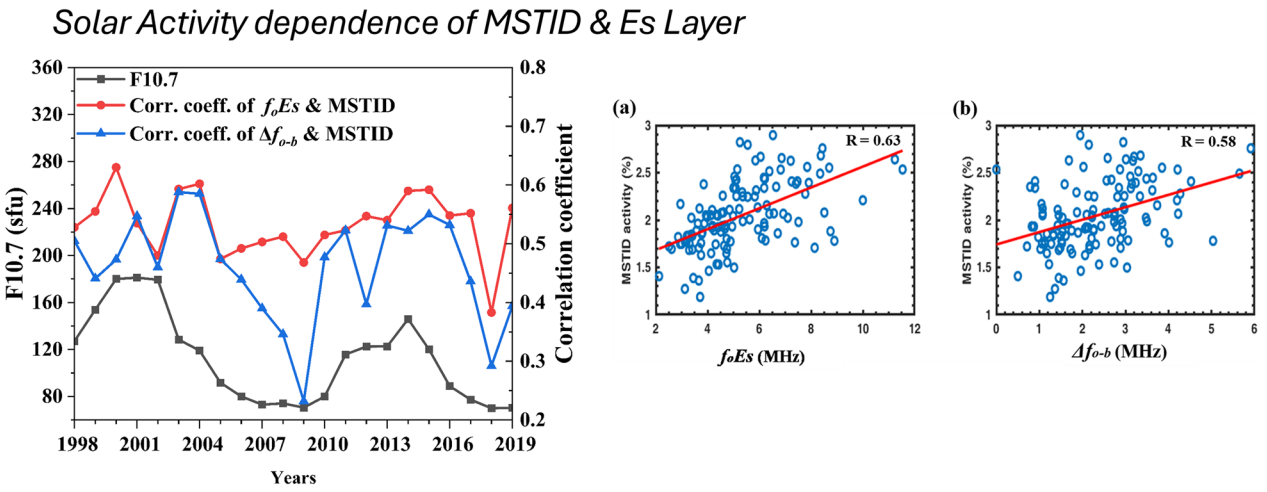

Introduction

Medium-scale traveling ionospheric disturbance (MSTID) is electron density perturbations in the F-region. The MSTID occurs at mid-latitudes as a manifestation of atmospheric gravity wave (AGW) in the daytime and due to electro-dynamic coupling in the nighttime (Kotake et al. 2007). Numerous characteristics of MSTID have been discovered since the late 1990s using ionospheric inferences using two-dimensional mapping techniques using all-sky airglow imagers and multipoint GPS receiver networks. Saito et al. (1998) utilized an extensive global positioning system (GPS) receiver network comprising approximately 1000 GPS receivers to generate two-dimensional map of total electron content (TEC) over Japan. They detected two-dimensional structure of the TEC perturbation induced by MSTID over Japan. The resulting TEC map emphasizes the valuable insight into the propagation behavior of MSTIDs, which has a southwestward direction during nighttime.

The nighttime MSTIDs propagate mostly southwestward in the northern hemisphere and northwestward in the southern hemisphere (Otsuka et al. 2004). The propagation direction of the nighttime MSTIDs is supporting the hypothesis that polarization electric fields might have a pivotal role in generating MSTIDs during nighttime (Shiokawa et al. 2003a; Saito et al. 2002; Kotake et al. 2007). Shiokawa et al. (2003b) investigated a nighttime MSTID measured by airglow observation at Shigaraki, Japan, and compared it with ion drift data of the DMSP F15 satellite and found that perturbations in the electric field are correlated with MSTID structures which have wave fronts aligned from northwest to southeast. Their findings revealed that the orientation of the electric field coincides with the polarization of the electric fields anticipated from the continuity of the electric current in the F region. These results suggests that the nighttime MSTIDs could be caused by the of the Perkins instability (Perkins 1973).

Kelley et al. (2003) proposed that the electrodynamical coupling between the E and F layers, stronger polarization electric fields, and perturbation in plasma density are enabling the role in development of nighttime MSTIDs. Saito et al. (2007) found a strong correlation between F region MSTID structures with E region field-aligned irregularities (FAIs). Otsuka et al. (2007) reported that the Doppler velocity of echoes from FAI in the *E* -region showed that the MSTID-induced airglow showed an enhancement (depletion) corresponding to southeastward (northwestward) velocity in the FAI echoes. These results show a significant relationship between the F region MSTID's electric fields and the *E* region's electric field perturbations.

At mid-latitudes, a Hall polarization process similar to the one fueling the equatorial electrojet can occur. The polarization electric fields produced by this mechanism may be stronger than the surrounding electric fields (e.g., Haldoupis et al. 1996). Tsunoda and Cosgrove (2001) have reported that the electric fields produced through the Hall polarization process in the *Es* layer could propagate into the F region, causing plasma density perturbations by amplifying the polarization electric fields. Cosgrove and Tsunoda (2002) have proposed a *Es* layer instability in which *Es* layer fluctuation grows when

the plasma density wavefronts align from northwest to southeast. Furthermore, Cosgrove and Tsunoda (2004) have put forward a coupling instability between the *Es* layer and F region, and shown that the coupling instability grows more rapidly than the Perkins instability alone.

Shalimov and Yamamoto (2010) proposed a simple quantitative model for mapping the polarization of the electric field within the F-region over the mid-latitude region. Their findings showed that polarization electric fields associated with *Es*, having sizes larger than 10 km, could effectively disturb the plasma in the F region at mid-latitudes. Several research findings has demonstrated that the interaction between the E and F regions can enhance the Perkins instability (Tsunoda and Cosgrove 2001; Cosgrove and Tsunoda 2004; Haldoupis et al. 2003; Cosgrove 2007, 2013; Otsuka et al. 2008; Earle et al. 2010; Hysell et al. 2018; Liu et al. 2019, 2020).

Otsuka et al. (2008) examined the coupling among the MSTID and status of *Es* layer events done with correlation statistics during the summer nights (May–August) of 2001–2005 using TEC data from a Japanese GPS network and ionosonde measurements taken at Kokubunji, Japan in May–August of 2001–2005. Their findings suggest that an electrodynamical coupling between *Es* and the F region via the polarization of the electric field could play an important role in generating nighttime MSTIDs and the spatial structure of *Es*. Since they analyzed the data only for 5 years from 2001 to 2005, they did not assert a solar activity dependence of the coupling between MSTID and *Es* layer. This study aims to disclose solar activity dependence of the coupling between MSTID activity and the *Es* layer by extending the period of the analyze data to 22 years from 1998 to 2019.

Data and methodology

Geospatial information authority of Japan (GSI) has been operating about 1000 dual frequency (L1 with 1.57542 GHz and L2 with 1.22760 GHz) GPS-receivers in Japan since 1999 (Sagiya et al. 2000). The carrier phase and pseudorange data at the dual-frequencies are obtained every 30 s. The carrier phase and pseudorange data of the dual-frequency GPS data are obtained every 30 s. Total electron content (TEC) along a ray path of the radio wave propagating from the GPS satellite to the receiver is obtained from the carrier phase and pseudorange data. TEC obtained from the carrier phase is more accurate than TEC from the pseudorange, but has an ambiguity due to the unknown initialization constant. The ambiguity was corrected by the TEC obtained from the corresponding pseudorange data. The inter-frequency biases included in the TEC obtained from the pseudorange were subtracted by using the method by Otsuka et al. (2002) to obtain absolute TEC.

For obtaining the perturbation in TEC due to MSTID, a 1-h running average has been subtracted from the time series of TEC obtained for each pair of satellites and receivers (Saito et al. 1998). To mitigate the multipath effect caused by obstacles surrounding the receivers, we used the data with satellite elevation angle higher than 35°. In this way, the obtained slant TEC is multiplied by a factor defined as $^{\tau_0}/_{\tau_1}$ to obtain the vertical TEC, where τ_1 is the distance travelled by the radio wave in the ionosphere spanning an altitude range from 250 to 450 km, and τ_0 is the vertical extent or depth of the ionosphere (200 km). This vertical detrended TEC values were mapped onto the ionospheric shell existing at an altitude of 300 km in the geographical coordinates with a grid size of 0.15° × 0.15° in longitude and latitude. The TEC values in each grid are averaged. This method to make two-dimensional maps of the detrended TEC is reported by (Saito et al. 1998).

According to Otsuka et al. (2008), the MSTID activity is defined as the ratio $^{\delta I}/_{\bar{I}} \times 100[\%]$, where δI represents the standard deviation of TEC perturbations observed in a specific region ranging from 33.75° N to 37.80° N and 137.50° E to 141.55° E over 1 h, and $\bar{I}$ denotes the background TEC obtained as an average of vertical TEC in the same area and during the corresponding time span as δI. The MSTID activity in summer (between May and August) from 1998 to 2019 was used in this study.

In this statistical study, the critical frequency (f_oEs) and blanketing frequency (f_bEs) of *Es* layer obtained by an ionosonde at Kokubunji (35.7° N, 139.5° E) in Japan during a period from 1998 and 2019 are analyzed. This study uses hourly values of manually scaled parameters provided by the World Data Centre (https://wdc.nict.go.jp) of the Institute of Information and Communications Technology (NICT). Since f_oEs represents the maximum and f_bEs represent minimum plasma frequencies in *Es* layer, respectively, the difference between the two plasma frequencies, $f_oEs - f_bEs \equiv \Delta f_{o-b}$ could indicate inhomogeneity of the concentration of denser plasma in Es Es layer (Ogawa et al. 2002). Although spatial scale of the inhomogeneity for the electron density in *Es* layer is considerably smaller than that of MSTIDs, temporal and day-to-day variations of Δf_{o-b} well correlate with those of the MSTID activity (Ogawa et al. 2002; Otsuka et al. 2008).

Results

Figure 1 represents daily variations of MSTID activity (brown curve) during nighttime, f_oEs(blue curve) and Δf_{o-b} (green curve) for the months of (a) May, (b) June, (c) July and (d). August of 2019. To derive the average values for each day, the f_oEs, Δf_{o-b} and MSTID activity are averaged over a period between 19:00 and 02:00 JST.

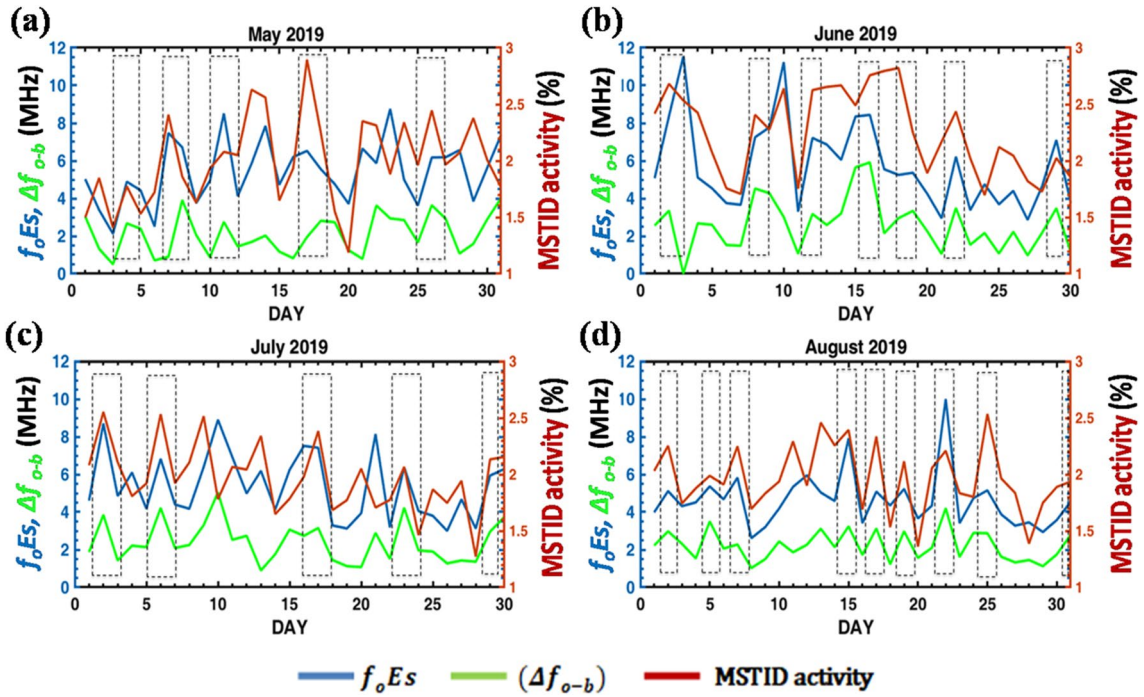

Fig. 1 Day-to-day variations of the nighttime averaged MSTID activity (brown), f_oEs(blue) and Δf_{o-b} (green) for **a** May, **b** June, **c** July and **d** August of 2019

From the figure, it is found that MSTID activity exhibits a rise on specific dates: May 4, 7, 11, 17 and 26, as well as June 2, 8, 12, 16, 18, 22 and 30 and further on July 2, 6, 17, 23 and 29, as well as August 2, 5, 7, 15, 17, 19, 22, 25 and 31. This increase corresponds with both *Es* parameters (f_oEs and Δf_{o-b}) also increasing, indicating a positive connection between them. On other days (e.g., May 29, June 24, July 10 and August 28 in 2019), however, f_oEs and Δf_{o-b} are negatively correlated with the MSTID activity. On the whole, the MSTID activity tends to be positively correlated with f_oEs and Δf_{o-b}, though their correlation appears to be moderate.

A qualitative investigation of the correlation between MSTID activity and f_oEs and between the MSTID activity and Δf_{o-b} has been done. Figures 2a, b shows the scatter plot of the May–August summer nights average

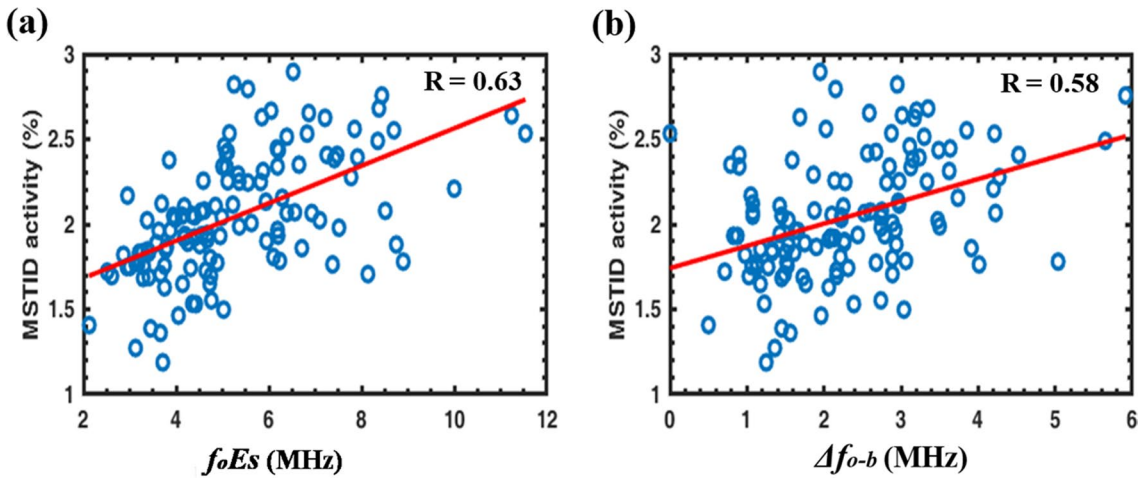

Fig. 2 Scatter plot of MSTID activity as a function of **a** f_oEs and **b** Δf_{o-b} and MSTID activity for May–August in 2019. A straight line in each figure represents the linear regression. Correlation coefficient (R) is also shown in each figure

of f_oEs and MSTID activity, and Δf_{o-b} and MSTID activity for 19–02 h (JST), respectively, for 2019. In the figures, a linear regression line is depicted to characterize the observed relationships. Based on the figures, it can be observed that there is a positive relationship between both f_oEs and Δf_{o-b} with the MSTID activity. The correlation coefficient of determination, denoted as R, serves as a metric to assess the adequacy of fit in a regression model. The correlation coefficient of determination (R) among MSTID and $f_oEs(\Delta f_{o-b})$ is 0.63 (0.58). This feature is consistent with that reported by Otsuka et al. (2008). In addition, we calculated the correlation coefficients between MSTID and $f_oEs(\Delta f_{o-b})$ for each year using the 22-year data from 1998 to 2019. Figure 3 shows the yearly variation of the correlation coefficient between f_oEs and MSTID activity, and between Δf_{o-b} and MSTID activity in summer nights of 19–02 h (JST) for 1998–2019. From 1998 to 2019, the correlation coefficients between MSTID and f_oEs (Δf_{o-b}) are 0.38–0.63 (0.23–0.58). F10.7 is also shown in Fig. 3 to investigate their solar activity dependence. The correlation coefficients between MSTID and f_oEs (Δf_{o-b}) in Fig. 3, depicting the 23rd and 24th solar cycles from 1998 to 2019, closely mirror the fluctuations in solar activity as represented by F10.7. During the ascending phase of the 23rd solar cycle in 1998, when F10.7 was at 118, the correlation coefficients between MSTID and $f_oEs(\Delta f_{o-b})$ were 0.25 (0.51). Similarly, in the peak year of 2000 when F10.7 rose to 180, the correlation coefficients between MSTID and $f_oEs(\Delta f_{o-b})$ increased to 0.63 (0.47). Conversely, in deep solar minimum year of 2005 when F10.7 declined to 92, the correlation coefficients between MSTID and $f_oEs(\Delta f_{o-b})$ also decreased to 0.47 (0.47), aligning with the solar activity trend. The 24th solar cycle, observed from 2008 to 2019, exhibited a similar pattern like 23rd solar cycle. During the ascending phase in 2010, with an F10.7 of 80, the correlation coefficients between MSTID and $f_oEs(\Delta f_{o-b})$ increased to 0.52 (0.47). In the peak year of 2014, when F10.7 reached 146, the correlation coefficients between MSTID and $f_oEs(\Delta f_{o-b})$ rose to 0.59 (0.52). Conversely, during the deep solar minimum year of 2018 and 2019 with an F10.7 of 70, the correlation coefficients between MSTID and f_oEs (Δf_{o-b}) decreased to 0.38 (0.29) and 0.56 (0.39) respectively, reflecting the solar activity trend. Hence, the correlation coefficients between MSTID and $f_oEs(\Delta f_{o-b})$ exhibit higher values during periods of high solar activity and lower values during periods of low solar activity. In brief, the correlation coefficients between MSTID

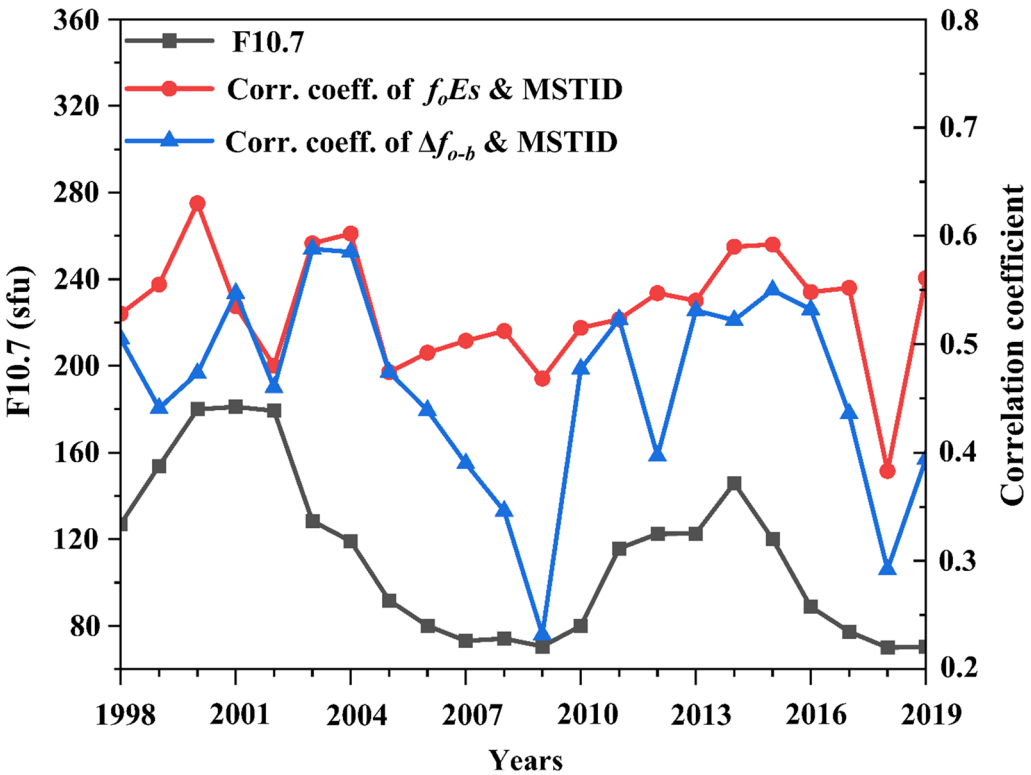

Fig. 3 Yearly variation of correlation coefficient between MSTID activity and f_oEs (red), and between MSTID activity and Δf_{o-b}(blue) averaged over summer nights of 19–02 h (JST) for the years of 1998–2019. F10.7 (black) is also shown in the figure

and $f_oEs(\Delta f_{o-b})$ closely follows the trend of solar activity represented by F10.7, highlighting their dependency on solar activity patterns.

Figure 4 shows the F10.7 dependence of the correlation coefficient between MSTID activity and f_oEs, and between MSTID activity and f_oEs for the summer nights of 19–02 h (JST) for 1998–2019. From Fig. 4, we find that the correlation coefficient of *Es* layer parameters and MSTID tend to increase with increasing solar activity, indicating that solar activity affects the E and F regions coupling process. It should be noted that during the low solar activity conditions, the correlation coefficient shows large variability.

Discussion

Our results show that that day-to-day variation of nighttime MSTIDs are well correlated with that of plasma density and its inhomogeneous structures in *Es* layer through all solar activity conditions. This result indicates that electrodynamical coupling processes between the *Es* layer and the F region along the geomagnetic fields could play an important role in generation of MSTIDs and inhomogeneities in the *Es* layer.

Mechanism for the nighttime MSTID generation can be explained in terms of the electrodynamical forces. The process of generating MSTIDs accompanying polarization electric fields are explained as follows (e.g., Otsuka et al. 2021). During the nighttime, the flow of the F region electric current ($\boldsymbol{J}$) in the northeastward direction is facilitated by the thermosphere neutral wind ($\boldsymbol{U}$), which issoutheastward. When $\boldsymbol{J}$ flows through the electron density perturbations, polarization electric fields ($\boldsymbol{E_p}$) are generated to maintain a divergence-free current density ($\boldsymbol{J}$). $\boldsymbol{E_p}$ is perpendicular to the wave fronts of MSTID, and oriented to the northeastward (southeastward) direction at the region where the height-integrated Pedersen conductivity is low (high). Due to upward and downward motion of the F-region plasma by oscillating $\boldsymbol{E_p} \times \boldsymbol{B}$ plasma drift, the electron density perturbations could be created, forming MSTIDs. The perturbations of the electron density and electric fields grow through the Perkins instability under the condition that the wave vector of MSTID falls between the eastward and $\boldsymbol{J}$ directions (Perkins 1973).

However, the growth rate of the Perkins instability alone is inadequate to explain the amplitude of the observed MSTID (e.g., Kelley et al. 2003). This expresses that MSTIDs cannot be generated solely via the Perkins instability. Cosgrove and Tsunoda (2002) have proposed another instability, which occurs in *Es* layer. It is referred to *Es* layer instability. It operates under the condition that the frontal structures of *Es* layer plasma densities have wave fronts aligned from northwest to southeast. Cosgrove and Tsunoda (2004) have proposed a coupling between the *Es* layer instability and Perkins instability, and reported that linear growth rate of the coupling instability is larger than that of the Perkins instability (Perkins 1973). Yokoyama et al. (2009), who have carried out three-dimensional simulations of the coupled Perkins and Es layer instabilities, conclude that the Es layer instability plays a major role in seeding NW–SE structure in the F region, and the Perkins instability is required to amplify its perturbations. Our observations suggest that coupling processes between Es layer and F region could

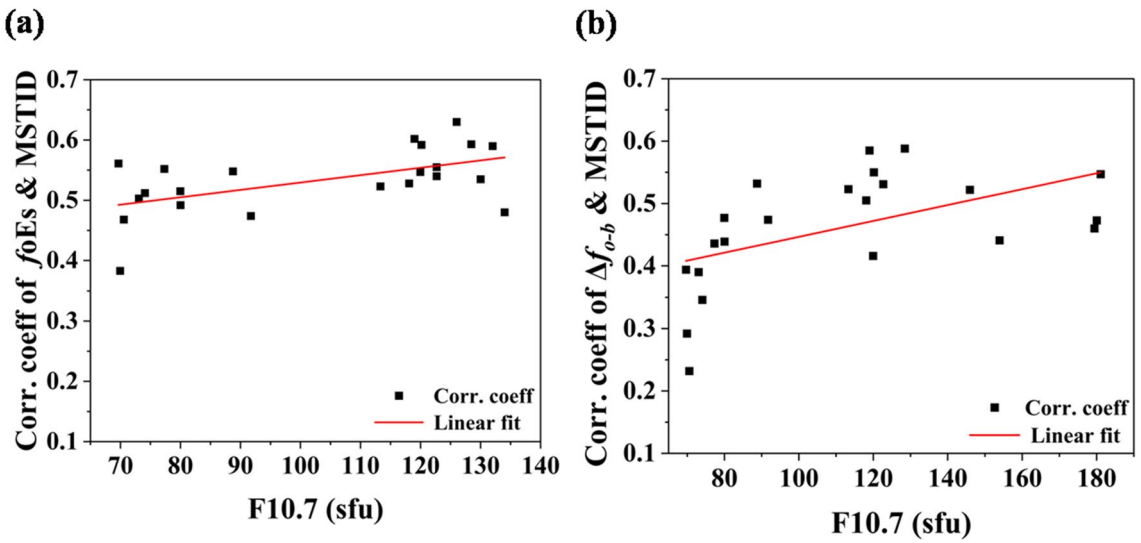

Fig. 4 F10.7 dependence of correlation coefficient between MSTID activity and **a** f_oEs and **b** Δf_{o-b} during the summer nights of 19–02 h (JST) for the years of 1998–2019

play an important role in day-to-day variations in the generation of the MSTIDs and E region disturbances.

Regarding the solar activity dependence of the instabilities, the growth rate of the Perkins instability is anticorrelated with the solar activity. This is because the growth rate of the Perkins instability is inversely proportional to the neutral density, which increases with the solar activity. Airglow and GPS–TEC observations show that occurrence rate of the MSTID and MSTID activity defined as a ratio of the amplitude of perturbed TEC to the background TEC shows anti-correlation with the solar activity (Takeo et al. 2017; Otsuka et al. 2021). The correlation coefficient between MSTID activity and f_oEs and between MSTID activity and Δf_{o-b} shows large variability during the low solar activity conditions, as shown in Fig. 4. This feature can be interpreted as follows: The Perkins instability is more effective during low solar activity than during high solar activity because the growth rate of the Perkins instability increases with decreasing solar activity. The growth rate of the Perkins instability is a function of the background neutral winds. Day-to-day variation of the Perkins instability growth rate could be controlled mainly by the background neutral winds.

In order to investigate solar activity dependence of *Es* layer, Fig. 5 shows the yearly variation of f_oEs and Δf_{o-b} averaged over summer nights of 19–02 h (JST). From 1998 to 2019, f_oEs ranges from 3.9 to 5.4, and Δf_{o-b} from 1.1 to 2.4. In the figure, yearly variation of F10.7 is also shown. Comparing f_oEs and Δf_{o-b} with F10.7, it is found that both f_oEs and Δf_{o-b} do not show distinct solar activity dependence. This feature is consistent with previous work done at mid latitudes by Pietrella and Bianchi (2009). This is probably because the *Es* layer is formed mainly by wind shear mechanism (Whitehead 1960). Yokoyama et al. (2009), who have carried out three-dimensional simulations for the coupling processes between the Perkins and *Es* layer instabilities, report that the *Es* layer instability plays a major role in seeding the perturbations elongating from northwest to southeast and that the Perkins instability amplify the perturbations. The current study shows that the correlation coefficient between the MSTID activity and *Es* layer

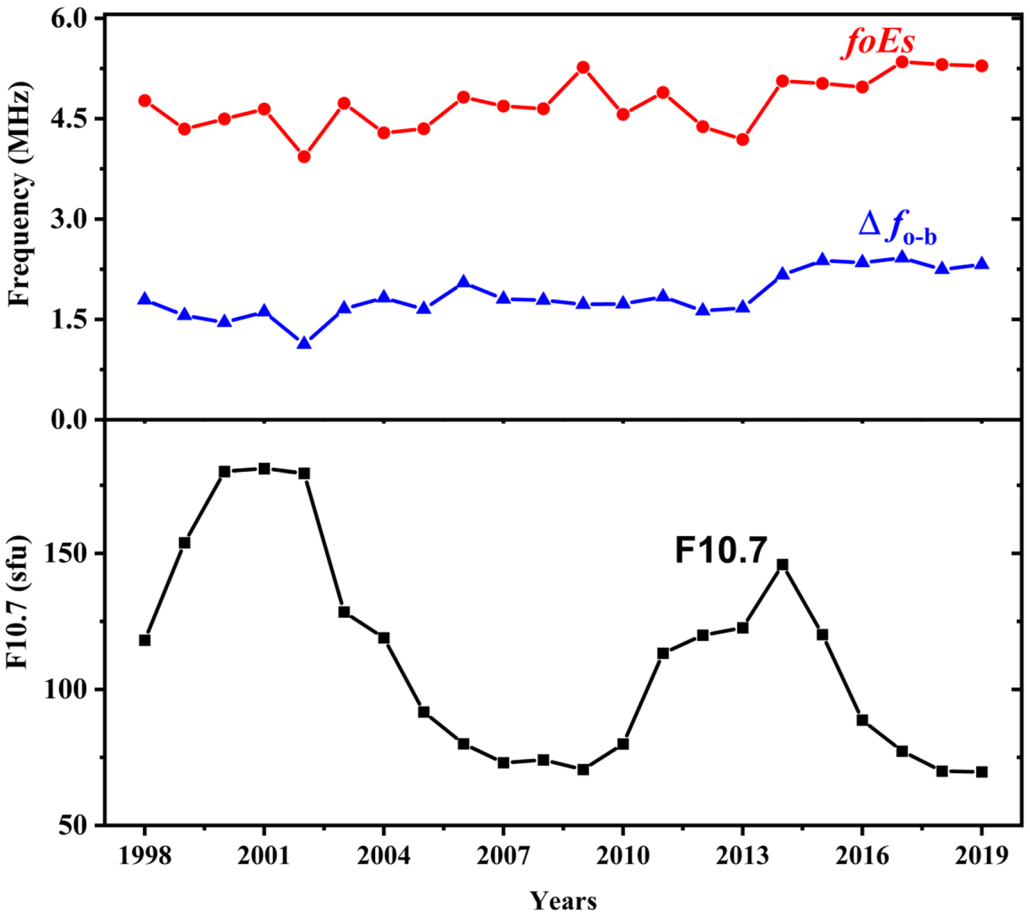

Fig. 5 Yearly variation of f_oEs(red) and Δf_{o-b} (blue) in summer nights of 19–02 h (JST) for the years of 1998–2019. F10.7 (black) is also shown in the figure

is positively correlated with the solar activity. Considering the previous studies mentioned above, the current result suggests that under the low solar activity conditions, when the growth rate of the Perkins instability is higher, MSTIDs could grow mainly through the Perkins instability even with weak seeding by the *Es* layer instability. On the other hand, under the high solar activity conditions, since the growth rate of the Perkins instability is smaller, seeding by the *Es* layer instability is needed for the MSTID growth. Consequently, the coupling between the MSTID and *Es* layer is intense under the high solar activity conditions.

Conclusion

We analyzed TEC data from the Japanese GPS network and ionosonde measurements taken at Kokubunji (35.7° N, 139.5° E), Japan, between May and August 1998–2019. Our objective is to explore the connection between the nighttime MSTIDs and *Es* layer. The obtained results regarding the correlation coefficient between the MSTID activities and f_oEs, Δf_{o-b} are summarized as follows:

1. Correlation coefficient between the MSTID activity and $f_oEs\left(\Delta f_{o-b}\right)$ is 0.53 (0.46) on average for a period from 1998 to 2019. These finding implies that the electrodynamical coupling between the *Es* layer and F region could play an important role in growing MSTIDs.

2. The correlation coefficient tends to increase with increasing solar activity. Considering that the Perkins instability growth rate decreases with increasing solar activity, we can speculate that under high solar activity conditions, when the growth rate of the Perkins instability is relatively low, seeding of polarization electric field perturbations in *Es* layer is vital in growing MSTIDs.

Abbreviations

AGW	Atmospheric Gravity Wave
FAI	Field-Aligned Irregularity
GPS	Global Positioning System
MSTID	Medium-scale travelling ionospheric disturbance
TEC	Total electron content
JST	Japan Standard Time

Acknowledgements

The Geospatial Information Authority of Japan provided the GPS data of Japan. The GPS–TEC data are archived by the National Institute of Information and Communications Technology (NICT), Japan. Acknowledgements to WDC, for ionosphere and space weather, Tokyo, NICT for providing ionosonde data. Mr. VeeraKumar Maheswaran acknowledges SCOSTEP for the travel support. The authors thank Omniweb (NASA) for providing F10.7 parameters. Mr. Veera-Kumar Maheswaran makes acknowledgement to Prof. R. Ramabadran (Rtd), H. O. D of Physics, GTN Arts College, Dindigul, India and Dr K.V. Balasubramanian, a retired meteorologist, IMD, Chennai, India for their continuous encouragement and inspiration all through his carrier.

Author contributions

Veera Kumar Maheswaran: problem design and formulation, Data analysis, Results and discussion and Manuscript writing. Yuichi Otsuka, Atsuki Shinbori, Takuya Sori, Michi Nishioka, Septi Perwitasari: problem design and formulation, Data support, suggested and verified the results and discussion. James A Baskaradas, S. Sriram, D. Venkata Ratnam: manuscript discussion and corrections, technical support and guidelines.

Funding

This work is supported by JSPS KAKENHI Grant Number 22K21345, JSPS Bilateral Joint Research Projects no. JPJSBP120226504, and JSPS Core-to-Core Program, B. Asia–Africa Science Platforms. Veera Kumar Maheswaran was supported by SCOSTEP SVS Award-2022.

Availability of data and materials

The GPS–TEC data are available at DRAWING–TEC (https://aer-nc-web.nict.go.jp/GPS/DRAWING-TEC/). The ionosonde data in Japan are available at https://wdc.nict.go.jp/IONO/HP2009/ISDJ/index-E.html.

Declarations

Ethics approval and consent to participate

Not applicable.

Consent for publication

Not applicable.

Competing interests

The authors declare no competing of interest.

Author details

[1]SASTRA Deemed University, Thanjavur 613401, India. [2]Institute for Space-Earth Environmental Research, Nagoya University, Nagoya, Japan. [3]Koneru Lakshamaiah Education Foundation, Vaddeswaram, Guntur 522502, India. [4]National Institute of Information and Communications Technology, Tokyo, Japan.

Received: 5 June 2023 Accepted: 30 April 2024
Published online: 21 June 2024

References

Cosgrove RB (2007) Generation of mesoscale F layer structure and electric fields by the combined Perkins and Es layer instabilities, in simulations. Ann Geophys 25:1579–1601. https://doi.org/10.5194/angeo-25-1579-2007

Cosgrove R (2013) Mechanisms for E-F coupling and their manifestation. J Atmos Solar-Terrestrial Phys 103:56–65. https://doi.org/10.1016/j.jastp.2013.03.011

Cosgrove RB, Tsunoda RT (2002) A direction-dependent instability of sporadic-E layers in the nighttime midlatitude ionosphere. Geophys Res Lett 29:1–4. https://doi.org/10.1029/2002gl014669

Cosgrove RB, Tsunoda RT (2004) Instability of the E-F coupled nighttime midlatitude ionosphere. J Geophys Res Sp Phys 109:1–7. https://doi.org/10.1029/2003JA010243

Earle GD, Bhaneja P, Roddy PA et al (2010) A comprehensive rocket and radar study of midlatitude spread F. J Geophys Res Sp Phys 115:1–21. https://doi.org/10.1029/2010JA015503

Haldoupis C, Schlegel K, Farley DT (1996) An explanation for type 1 radar echoes from the mid latitude E-region ionosphere. Geophys Res Lett 23:97–100. https://doi.org/10.1029/95GL03585

Haldoupis C, Kelley MC, Hussey GC, Shalimov S (2003) Role of unstable sporadic-E layers in the generation of midlatitude spread F. J Geophys Res Sp Phys 108:1–8. https://doi.org/10.1029/2003JA009956

Hysell D, Larsen M, Fritts D et al (2018) Major upwelling and overturning in the mid-latitude F region ionosphere. Nat Commun. https://doi.org/10.1038/s41467-018-05809-x

Kelley MC, Haldoupis C, Nicolls MJ et al (2003) Case studies of coupling between the E and F regions during unstable sporadic-E conditions. J Geophys Res Sp Phys. https://doi.org/10.1029/2003JA009955

Kotake N, Otsuka Y, Ogawa T et al (2007) Statistical study of medium-scale traveling ionospheric disturbances observed with the GPS networks in

Southern California. Earth, Planets Space 59:95–102. https://doi.org/10.1186/BF03352681
Liu Y, Zhou C, Tang Q et al (2019) Evidence of mid-and low-latitude nighttime ionospheric E-F Coupling: coordinated observations of sporadic E Layers, F-Region Field-aligned irregularities, and medium-scale traveling ionospheric disturbances. IEEE Trans Geosci Remote Sens 57:7547–7557. https://doi.org/10.1109/TGRS.2019.2914059
Liu Y, Zhou C, Xu T et al (2020) Investigation of midlatitude nighttime ionospheric E-F coupling and interhemispheric coupling by using COSMIC GPS radio occultation measurements. J Geophys Res Sp Phys 125:1–16. https://doi.org/10.1029/2019JA027625
Ogawa T, Takahashi O, Otsuka Y et al (2002) Simultaneous middle and upper atmosphere radar and ionospheric sounder observations of midlatitude E region irregularities and sporadic E layer. J Geophys Res Sp Phys 107:1–13. https://doi.org/10.1029/2001JA900176
Otsuka Y, Ogawa T, Saito A et al (2002) A new technique for mapping of total electron content using GPS network in Japan. Earth, Planets Space 54:63–70. https://doi.org/10.1186/BF03352422
Otsuka Y, Shiokawa K, Ogawa T, Wilkinson P (2004) Geomagnetic conjugate observations of medium-scale traveling ionospheric disturbances at midlatitude using all-sky airglow imagers. Geophys Res Lett. https://doi.org/10.1029/2004GL020262
Otsuka Y, Onoma F, Shiokawa K et al (2007) Simultaneous observations of nighttime medium-scale traveling ionospheric disturbances and e region field-aligned irregularities at midlatitude. J Geophys Res Sp Phys 112:1–9. https://doi.org/10.1029/2005JA011548
Otsuka Y, Tani T, Tsugawa T et al (2008) Statistical study of relationship between medium-scale traveling ionospheric disturbance and sporadic E layer activities in summer night over Japan. J Atmos Solar-Terrestrial Phys 70:2196–2202. https://doi.org/10.1016/j.jastp.2008.07.008
Otsuka Y, Shinbori A, Tsugawa T, Nishioka M (2021) Solar activity dependence of medium-scale traveling ionospheric disturbances using GPS receivers in Japan. Earth, Planets Space. https://doi.org/10.1186/s40623-020-01353-5
Perkins F (1973) Spread F and ionospheric currents. J Geophys Res 78:218–226. https://doi.org/10.1029/ja078i001p00218
Pietrella M, Bianchi C (2009) Occurrence of sporadic-E layer over the ionospheric station of Rome: analysis of data for thirty-two years. Adv Sp Res 44:72–81. https://doi.org/10.1016/j.asr.2009.03.006
Sagiya T, Miyazaki S, Tada T (2000) Continuous GPS array and present-day crustal deformation of Japan. Pure Appl Geophys 157:2303–2322. https://doi.org/10.1007/978-3-0348-7695-7_26
Saito A, Fukao S, Miyazaki S (1998) High resolution mapping of TEC perturbations with the GSI GPS network over Japan. Geophys Res Lett 25:3079–3082. https://doi.org/10.1029/98GL52361
Saito A, Nishimura M, Yamamoto M et al (2002) Observations of traveling ionospheric disturbances and 3-m scale irregularities in the nighttime F-region ionosphere with the MU radar and a GPS network. Earth, Planets Space 54:31–44. https://doi.org/10.1186/BF03352419
Saito S, Yamamoto M, Hashiguchi H et al (2007) Observational evidence of coupling between quasi-periodic echoes and medium scale traveling ionospheric disturbances. Ann Geophys 25:2185–2194. https://doi.org/10.5194/angeo-25-2185-2007
Shalimov S, Yamamoto M (2010) Influence of midlatitude sporadic E layer patches upon the F region plasma density. J Geophys Res Sp Phys 115:1–7. https://doi.org/10.1029/2009JA014964
Shiokawa K, Ihara C, Otsuka Y, Ogawa T (2003a) Statistical study of nighttime medium-scale traveling ionospheric disturbances using midlatitude airglow images. J Geophys Res Sp Phys 108:1–7. https://doi.org/10.1029/2002JA009491
Shiokawa K, Otsuka Y, Ihara C et al (2003b) Ground and satellite observations of nighttime medium-scale traveling ionospheric disturbance at midlatitude. J Geophys Res Sp Phys 108:1–13. https://doi.org/10.1029/2002JA009639
Takeo D, Shiokawa K, Fujinami H et al (2017) Sixteen year variation of horizontal phase velocity and propagation direction of mesospheric and thermospheric waves in airglow images at Shigaraki, Japan. J Geophys Res Sp Phys 122:8770–8780. https://doi.org/10.1002/2017JA023919
Tsunoda RT, Cosgrove RB (2001) Coupled electrodynamics in the nighttime midlatitude ionosphere. Geophys Res Lett 28:4171–4174. https://doi.org/10.1029/2001GL013245
Whitehead JD (1960) Formation of the Sporadic E Layer in the Temperate Zones. Nature 188:4780
Yokoyama T, Hysell DL, Otsuka Y, Yamamoto M (2009) Three-dimensional simulation of the coupled Perkins and es-layer instabilities in the nighttime midlatitude ionosphere. J Geophys Res Sp Phys 114:1–16. https://doi.org/10.1029/2008JA013789

Publisher's Note